

# Biologically inspired oxidation catalysis

Lawrence Que Jr<sup>1</sup> & William B. Tolman<sup>1</sup>

**The development of processes for selective hydrocarbon oxidation is a goal that has long been pursued. An additional challenge is to make such processes environmentally friendly, for example by using non-toxic reagents and energy-efficient catalytic methods. Excellent examples are naturally occurring iron- or copper-containing metalloenzymes, and extensive studies have revealed the key chemical principles that underlie their efficacy as catalysts for aerobic oxidations. Important inroads have been made in applying this knowledge to the development of synthetic catalysts that model enzyme function. Such biologically inspired hydrocarbon oxidation catalysts hold great promise for wide-ranging synthetic applications.**

The selective oxidation of organic molecules is fundamentally important to life and immensely useful in industry<sup>1,2</sup>. Among the myriad ways by which such reactions may be performed, those catalysed by naturally occurring metalloenzymes using molecular oxygen (O<sub>2</sub>) are notable for many reasons. Metalloenzyme-catalysed oxidations often exhibit exquisite substrate specificity as well as regioselectivity and/or stereoselectivity, and operate under mild conditions through inherently 'green' processes. Moreover, metalloenzymes are sometimes able to alter the function of recalcitrant substrates in ways that synthetic chemists find difficult to replicate (for example, changing methane to methanol)<sup>1,3</sup>. For these reasons, combined with the knowledge that metal centres in proteins often adopt novel structures and exhibit unusual properties that are intrinsically worth examining, bioinorganic chemists have studied O<sub>2</sub>-activating metalloenzyme structure–function relationships extensively.

Significant advances in our understanding of how these enzymes function have accrued, in part from the high-resolution structures of resting states and reactive metalloenzyme intermediates through X-ray crystallography and spectroscopic characterization, and from detailed mechanistic information from intertwined kinetics, synthetic modelling and theoretical investigations. Such studies have produced candidates for the active oxidants in several classes of important copper and iron enzymes that are the subject of this review. These findings have fuelled the debate about the mechanisms by which these enzymes operate; one common issue being whether O–O bond cleavage occurs before, during or after attack on the organic substrate.

Although valuable in its own right, an added benefit of knowing the metalloenzyme structure and function is its potential application in the design of synthetic catalysts. Such 'bioinspired' or 'biomimetic' catalysts<sup>4,5</sup> may have an advantage over metalloenzyme systems, insofar as they might expand the scope of possible substrates, increase the scale of production and tune selectivity and/or specificity (for example, reversal of asymmetric induction in a stereoselective process). They would also be useful for environmentally friendly catalytic chemistry<sup>6</sup>, where it is important to avoid the use of toxic or expensive metal reagents and oxidants, energy-consuming processing steps and undesirable reaction media. Furthermore, mechanistic studies of biomimetic catalysts can provide important insights into biological pathways, thus completing a feedback loop relating studies of metalloenzymes to their synthetic models. Indeed, recent advances in the design of biologically inspired oxidation catalysts containing inexpensive and readily available iron and copper centres have led to a new understanding of the fundamental

reaction steps and reactive intermediates relevant to metalloenzymes that incorporate these metals in their active sites, as well as to practical applications. In this review, we survey several examples of these advances, with particular emphasis in each case on the interplay of catalyst design and knowledge of metalloenzyme structure and function.

## Biochemical inspirations

Iron and copper ions are the metal ions of choice for many biological oxidations because of their abundance in the geosphere, inherent electronic properties and accessible redox potentials. Pertinent examples are enzymes that contain haem iron, non-haem iron and copper active sites.

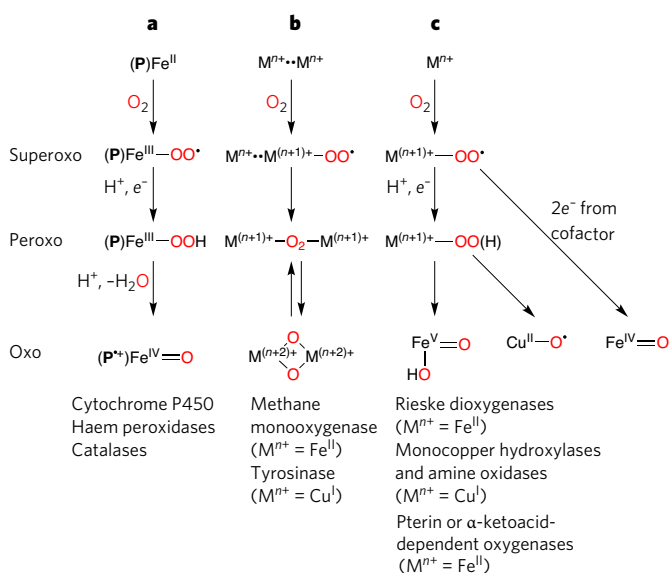


**Figure 1 | Metallo-oxygenase mechanisms.** To emphasize parallels with the haem paradigm (**a**), mechanisms proposed for O<sub>2</sub> activation by various metallo-oxygenases — di-iron and dicopper (**b**), and mononuclear non-haem iron and copper (**c**) — are shown. All involve the formation of an initial O<sub>2</sub> adduct (superoxo), conversion to a metal–peroxide (peroxo), and subsequent O–O bond cleavage to yield a high-valent oxidant (oxo). Oxygen atoms involved in these processes are shown in red. *e*<sup>−</sup>, electron; M, metal; P, porphyrin.

<sup>1</sup>Department of Chemistry and Center for Metals in Biocatalysis, University of Minnesota, 207 Pleasant Street SE, Minneapolis, Minnesota 55455, USA.

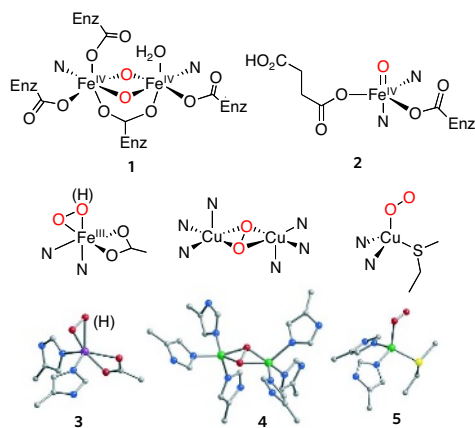


**Figure 2 | Metalloenzyme intermediates.** Diverse  $O_2$ -derived metalloenzyme intermediates have been proposed on the basis of spectroscopic and theoretical investigations (1 and 2) and have been structurally characterized by X-ray crystallography (3–5). Species 1 is postulated to hydroxylate methane in soluble methane monooxygenase, whereas 2 is proposed to be the active oxidant in the non-haem iron  $\alpha$ -ketoacid-dependent enzymes. Species 3 is an oxygenated intermediate from naphthalene dioxygenase; 4 is the  $(\mu-\eta^2:\eta^2)$ -peroxo dicopper(II) core of oxy-tyrosinase (akin to that identified in haemocyanin and catechol oxidase); and 5 is an  $O_2$  adduct identified in peptidylglycine  $\alpha$ -hydroxylating monooxygenase. For clarity, histidine imidazolyl donor ligands are indicated by N. Key oxygen atoms involved in these processes are shown in red. In the molecular models, carbon is shown in grey, oxygen in red, nitrogen in blue, copper in green, sulphur in yellow and iron in purple. Enz, enzyme.

### The haem paradigm

The most extensively studied oxygen-activating enzymes are the cytochromes P450 (ref. 7). They carry out the hydroxylation of aliphatic C–H bonds and the epoxidation of C=C double bonds (C=C bonds) with high regioselectivity and stereoselectivity. Cytochromes P450 have an active site that consists of an iron porphyrin cofactor attached to the protein backbone through coordination of a cysteine at one of the axial positions on the metal, leaving the other axial position available for  $O_2$  binding and activation. Related haem peroxidases and catalases activate peroxides with similar active sites where the axial cysteine is replaced by histidine or tyrosine<sup>8</sup>.

The activation of  $O_2$  at a metal centre generally entails its two-electron reduction to the peroxo state and subsequent O–O bond cleavage.

The generally accepted oxygen activation mechanism associated with cytochrome P450 is referred to as the haem paradigm<sup>9</sup> (Fig. 1a). In the initial step,  $O_2$  coordinates to the reduced iron centre. It becomes progressively reduced to superoxo and peroxo forms and undergoes O–O bond cleavage to generate a formally oxoiron(v) oxidant that carries out the two-electron oxidation of the substrate. For haem enzymes, the two oxidizing equivalents required for oxidation are not stored at the iron centre but are instead delocalized on the iron porphyrin unit, so the formally oxoiron(v) oxidant in haem enzymes is generally described as an oxoiron(IV)-(oxidized porphyrin radical) species. Such delocalization allows access to a potent oxidant that is competent to attack a variety of substrates, a common strategy in biocatalysis that informs biomimetic design efforts.

### Non-haem iron enzymes

As outlined in Fig. 1, the proposed mechanisms for non-haem iron enzymes in general follow the haem paradigm, and evidence for iron(III)–peroxo and high-valent iron–oxo intermediates has been obtained for some of these enzymes. For example, the di-iron enzyme methane monooxygenase (MMO)<sup>10</sup> that catalyses the conversion of methane to methanol activates  $O_2$  via di-iron(III)–peroxo and di-iron(IV) intermediates (Fig. 1b). Although the former has been implicated as the oxidant in the epoxidation of electron-rich alkenes such as ethyl vinyl ether<sup>11</sup>, the latter has been demonstrated to be kinetically competent to hydroxylate methane<sup>12</sup>. This di-iron(IV) species has been shown by extended X-ray absorption fine structure (EXAFS) analysis to have a  $di(\mu\text{-oxo})di\text{-iron(IV)}$  core<sup>13</sup> (1, Fig. 2).

The Rieske dioxygenases, by contrast, activate  $O_2$  at a mononuclear iron centre bound to a 2-His-1-carboxylate facial triad motif<sup>14</sup> (Fig. 1c). These enzymes catalyse the *cis*-dihydroxylation of arene double bonds to initiate the biodegradation of aromatics in the soil. For these enzymes, the only redox centre that can store the two required oxidizing equivalents is the iron atom, so an oxoiron(v) oxidant has been invoked for this reaction. Although direct evidence for a non-haem oxoiron(v) species in the enzyme cycle has not yet been obtained, its iron(III)–peroxo precursor (3, Fig. 2) has been characterized by X-ray crystallography<sup>15</sup>. It is proposed that the side-on peroxo moiety either attacks the arene double bond directly or isomerizes first to an oxo(hydroxo)iron(v) species. Several examples of oxoiron(IV) intermediates (2, Fig. 2) have been trapped and characterized<sup>16</sup> in studies of non-haem iron enzymes that use organic cofactors such as  $\alpha$ -ketoglutarate or tetrahydrobiopterin, lending credence to the general mechanistic scheme presented in Fig. 1. Importantly, each of the side-on peroxo, oxoiron(v) or oxoiron(IV) species postulated for the non-haem iron enzymes is a viable target for the development of biologically inspired catalysts.

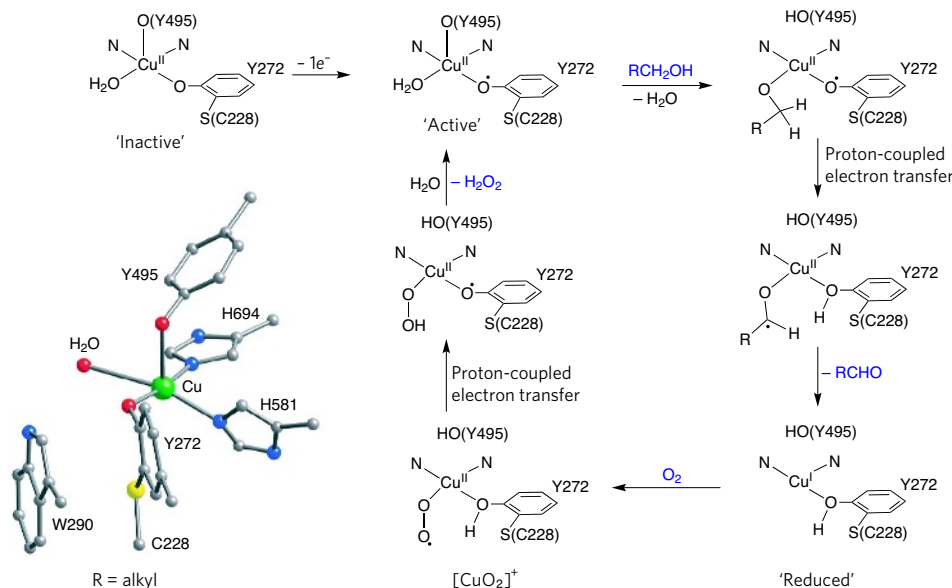


**Figure 3 | Galactose oxidase mechanism.**

The X-ray structure for the 'inactive' form of galactose oxidase (GAO) (Protein Data Bank identity 1GOG)<sup>20</sup> illustrates the disposition of ligands in the active site of the enzyme. Important components of the proposed mechanism for this enzyme include the involvement of the Cu(II)-tyrosyl radical unit ('active') in alcohol oxidation through intramolecular proton-coupled electron transfer. This unit is regenerated from a Cu(I) intermediate that reacts with  $O_2$  to yield a  $[CuO_2]^+$  species, which evolves  $H_2O_2$  via another proton-coupled electron-transfer process. For clarity, histidine imidazolyl donor ligands are indicated by N. Organic substrates and products are shown in blue. In the molecular models, carbon is shown in grey, oxygen in red, nitrogen in blue, copper in green and sulphur in yellow.

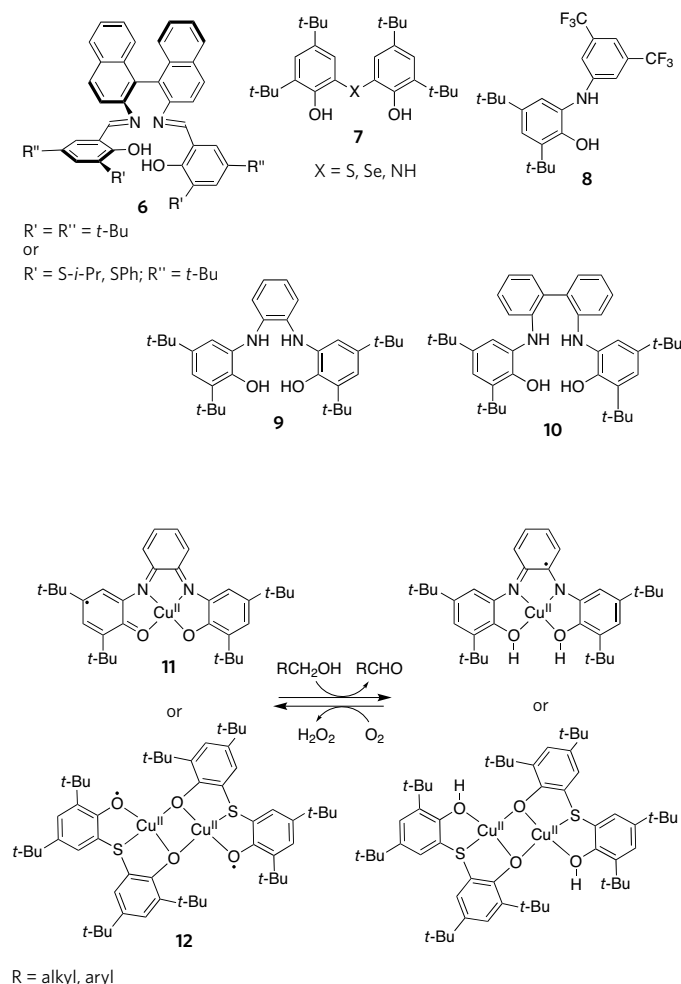


**Figure 4 | Ligands for modelling GAO.** Deprotonated versions of the ligands 6–10 have been used to prepare copper complexes that mimic GAO function, insofar as they catalyse the aerobic oxidation of alcohols to aldehydes or ketones via the intermediacy of Cu(II)-phenoxyl radical species and produce H<sub>2</sub>O<sub>2</sub> as a coproduct. Synthetic Cu(II)-phenoxyl radical complexes of differing nuclearity (11 and 12) catalytically oxidize alcohols just as GAO does, but without the apparent involvement of a Cu(I) intermediate; instead, only ligand-centred redox reactions have been suggested to occur. *i*-Pr, isopropyl; Ph, phenyl; *t*-Bu, *tert*-butyl.

### Copper enzymes

Copper-containing oxidases and oxygenases comprise a large class of enzymes that use intriguing mechanisms to bind and activate O<sub>2</sub> and oxidize organic substrates<sup>17</sup>. The active sites of these enzymes contain varying numbers of copper ions, and they have diverse structures that underlie similarly diverse functional attributes. We focus here on a select few for which extensive structure and function information has been obtained and applied to the development of biomimetic catalysts.

Galactose oxidase (GAO) is a well-studied member of the family of radical copper oxidases that use a novel copper(II)-tyrosyl radical unit to perform two-electron redox chemistry<sup>18,19</sup>. GAO couples the reduction of O<sub>2</sub> to H<sub>2</sub>O<sub>2</sub> with the oxidation of primary alcohols to aldehydes. As shown by X-ray crystallography (Fig. 3), the so-called 'inactive' form of GAO features an unusual tyrosinate ligand (at amino acid 272 of the enzyme (Y272)) covalently linked to a cysteine (C228)<sup>20</sup>. In the 'active' form of the enzyme, this ligand exists as a one-electron oxidized tyrosyl radical that is stabilized by a nearby tryptophan<sup>21</sup> (W290). In the consensus mechanism (Fig. 3), the 'active' Cu(II)–Y272• form is responsible for alcohol oxidation in one phase of the catalytic cycle. It is regenerated, with production of H<sub>2</sub>O<sub>2</sub>, in the second phase by reaction of the resulting

'reduced' Cu(I) form with O<sub>2</sub>. Many details of these processes have been elucidated through studies of the enzyme, synthetic modelling<sup>22,23</sup> and theoretical calculations<sup>24</sup>, including dissection of the key C–H bond-activating process into electron transfer, proton transfer and H-atom abstraction components using kinetic isotope effects and quantitative structure-activity relationship correlations<sup>25</sup>. Notably, the coupling of the one-electron redox cycles, Cu(I) ↔ Cu(II) and Y272 ↔ Y272•, to effect the overall two-electron catalytic half-reaction uniquely illustrates metal and organic cofactor synergism worthy of incorporation into designs of synthetic oxidation catalysts.

Tyrosinase and catechol oxidase use an oxidant entirely different from the Cu(II)-tyrosyl radical. In common with the reversible O<sub>2</sub> carrier protein haemocyanin, the dicopper(I) active sites of tyrosinase and catechol oxidase react with O<sub>2</sub> to generate a (peroxo)dicopper(II) unit that features an unusual side-on (μ-η<sup>2</sup>:η<sup>2</sup>) binding mode, as shown by X-ray crystallography for haemocyanin<sup>26,27</sup> and tyrosinase<sup>28</sup> and by spectroscopy for catechol oxidase<sup>29</sup> (4, Fig. 2). The μ-η<sup>2</sup>:η<sup>2</sup>-peroxide has an O–O stretching frequency (~750 cm<sup>-1</sup>) lower than that of most metal-peroxide complexes (850–900 cm<sup>-1</sup>), suggesting significant activation of the dioxygen O–O bond by its side-on coordination to two Cu(II) ions. The (μ-η<sup>2</sup>:η<sup>2</sup>-peroxo)dicopper(II) unit is postulated to be responsible for the oxidation of phenols (by tyrosinase) and/or catechols (by catechol oxidase)<sup>17,30</sup>, the former occurring by an electrophilic aromatic substitution pathway<sup>31</sup>.

Numerous (peroxo)dicopper(II) complexes have been synthesized, including examples with (μ-η<sup>2</sup>:η<sup>2</sup>-peroxo)dicopper(II) cores<sup>32–34</sup>. Some of these interconvert with di(μ-oxo)dicopper(III) isomers (Fig. 1), raising the alternative possibility that this core is responsible for substrate attack during catalysis by tyrosinase or catechol oxidase (despite the fact that it has not yet been observed in a protein)<sup>35</sup>. Developing synthetic systems that can access either or both cores from O<sub>2</sub> is an important biomimetic strategy for preparing environmentally friendly oxidizing reagents.

Monocopper-oxygen species are implicated as intermediates in the functionally important enzymes amine oxidase (AO)<sup>36</sup>, dopamine β-monooxygenase (DβM) and peptidylglycine α-hydroxylating monooxygenase (PHM)<sup>37</sup>. Intermediates under consideration include [CuO<sub>2</sub>]<sup>+</sup>, [CuOOH]<sup>+</sup> and [CuO]<sup>+</sup> units (Fig. 1). Kinetic<sup>38</sup> and theoretical studies<sup>39</sup> have been interpreted to indicate that a [CuO<sub>2</sub>]<sup>+</sup> moiety attacks the substrate in PHM and DβM; such a core has been thoroughly defined in synthetic model complexes<sup>40</sup> and by X-ray crystallography for PHM (5, Fig. 2), although its charge is not known in this case<sup>41</sup>. Other theoretical studies suggest that the [CuO]<sup>+</sup> unit is a more potent oxidant potentially capable of attacking substrate in these enzymes<sup>42,43</sup>. Such a species has not been identified conclusively in an enzyme or synthetic complex, however; so its role in biological and synthetic systems remains controversial<sup>44</sup>. Still, the anticipated high oxidizing power of the [CuO]<sup>+</sup> moiety makes it an attractive target in efforts to design catalysts for the oxidation of relatively unreactive substrates.

### Biologically inspired catalysis

The results of the biochemical studies discussed here provide a useful starting point for the design of synthetic oxidation catalysts. Progress in this area is summarized in this section.

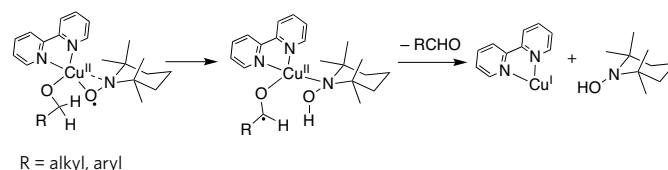


**Figure 5 | Copper-TEMPO radical oxidation.** The alcohol oxidation steps proposed for the bipyridine–Cu–TEMPO (Cu–2,2,6,6-tetramethyl-1-piperidinyloxy) system are closely related to those proposed for GAO (Fig. 3), despite the different chemical natures of the organic radical cofactors involved (that is, nitroxyl for Cu–TEMPO compared with phenoxyl for GAO).

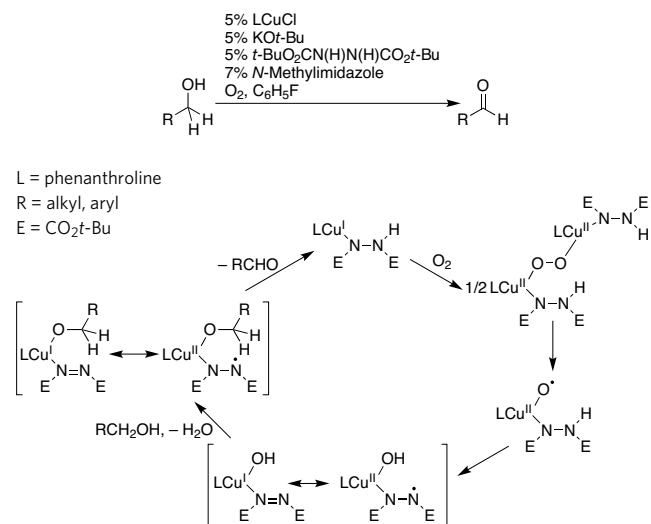


**Figure 6 | Proposed mechanism for alcohol oxidation.** An optimized system for the catalytic oxidation of a variety of alcohols is proposed to involve formation of a (peroxo)dicopper(II) complex that undergoes O–O bond homolysis to yield an intermediate with a [CuO]<sup>+</sup> core. Intramolecular hydrogen-atom abstraction is suggested to occur, followed by ligand substitution and subsequent aldehyde generation via a mechanism conceptually related to that followed by GAO and the Cu–TEMPO systems.

### Copper-catalysed alcohol oxidations

Within the broader context of copper-catalysed oxidations of hydrocarbons<sup>45</sup>, particular attention has been paid to the oxidation of alcohols to carbonyl compounds using O<sub>2</sub> as an oxidant. This is because of the significance of the transformation and the desire to develop ‘green’ alternatives to procedures that use heavy metal reagents or sensitive and/or expensive oxidants, and to procedures that are not economical or environmentally friendly<sup>46,47</sup>. Inspired by the coupling of an organic cofactor and Cu(I) ↔ Cu(II) redox chemistry in alcohol oxidation by the radical copper oxidases (for example, GAO), a variety of synthetic systems incorporating organic radicals and copper complexes have been studied for this reaction.

In direct analogy to the function of GAO, copper complexes of the deprotonated forms of the ligands **6–10** (Fig. 4) catalyse the aerobic oxidation of selected alcohols to aldehydes and/or ketones with concomitant generation of H<sub>2</sub>O<sub>2</sub> as a coproduct<sup>48–54</sup>. The involvement of Cu(II)–phenoxyl radical intermediates in these reactions is a further similarity with GAO, although differences in mechanism among the synthetic systems and the enzyme have been found. For instance, although the system derived from ligand **6** follows a pathway entirely analogous to that proposed for GAO involving cycling between Cu(II)–phenoxyl radical and Cu(I)–phenol intermediates<sup>48,49</sup>, complexes **11** (ref. 53) and **12** (ref. 51) follow mechanisms that do not involve changes in the metal-oxidation state and differ further with respect to the nuclearity of the proposed active species.

Conceptually related catalytic systems for the aerobic oxidation of alcohols incorporate copper salts and the 2,2,6,6-tetramethyl-1-piperidinyloxyl (TEMPO) radical<sup>46,55</sup>. A variety of copper salts, exogenous bases and reaction media (including environmentally friendly ionic liquids<sup>56</sup> or fluorinated biphasic systems<sup>57</sup>) have been used for this reaction, which differs from that of GAO insofar as H<sub>2</sub>O rather than H<sub>2</sub>O<sub>2</sub> is produced as the coproduct with the aldehyde or ketone. Nonetheless, pronounced mechanistic similarities with GAO are evident in some cases (Fig. 5), with TEMPO playing the same part as the phenoxyl radical in the enzyme.

Another versatile catalytic system combines CuCl, phenanthroline, a suitable base and a substituted hydrazine as the reducing agent<sup>58</sup>. The optimized conditions shown in Fig. 6 include *N*-methylimidazole as an additive and are useful for the clean oxidation of a variety of primary and

secondary alcohols to the respective ketones or aldehydes<sup>59</sup>. In common with the Cu–TEMPO systems, O<sub>2</sub> acts as stoichiometric oxidant and H<sub>2</sub>O is the sole byproduct. An intriguing mechanism has been proposed involving a [CuO]<sup>+</sup> species as an intermediate and a pathway for intramolecular oxidation of coordinated alkoxide that bears some resemblance to that proposed for GAO and the Cu–TEMPO systems.

### Copper-catalysed phenol and catechol oxidations

The oxidative reactivity of dicopper complexes that model the active sites of tyrosinase and catechol oxidase has been explored extensively in efforts aimed mostly at obtaining mechanistic insights into the activity of the enzymes<sup>33,34,60,61</sup>. With respect to understanding the phenolase activity of tyrosinase, emphasis has been placed on examining the involvement of the (μ-η<sup>2</sup>:η<sup>2</sup>-peroxo)dicopper(II) complexes and/or their di(μ-oxo)dicopper isomers in stoichiometric (non-catalytic) hydroxylations of ligand arene moieties and external phenols. In a catalytic application that capitalizes on the common observation of radical coupling of phenol substrates by these oxidants, tyrosinase model complexes have been used for the regio-controlled oxidative coupling polymerization of phenols<sup>62–66</sup> (Fig. 7a). Steric influences of the supporting ligand are thought to be critical in inhibiting undesired reactions at the *ortho* position in the putative Cu(II)–phenolate ↔ Cu(I)–phenoxyl intermediate, thus resulting in useful poly(1,4-phenylene ether) materials. Several dicopper complexes have also been studied as catalysts for the aerobic oxidation of catechols to *ortho*-quinones, which is analogous to catechol oxidase activity. In general, catechols may be oxidized both by dicopper(II) complexes and O<sub>2</sub> adducts such as (μ-peroxo)dicopper(II) species, and catalytic cycles incorporating both processes have been suggested that typically involve coordination of the catecholate to both copper ions and evolution of H<sub>2</sub>O and/or H<sub>2</sub>O<sub>2</sub> byproducts (Fig. 7b).

### Iron-catalysed hydrocarbon oxidations

A common feature of the catalytic cycles of cytochrome P450, MMO and the Rieske dioxygenases is the involvement of an iron(III)–peroxo intermediate (Fig. 1). This intermediate may react directly with the substrate

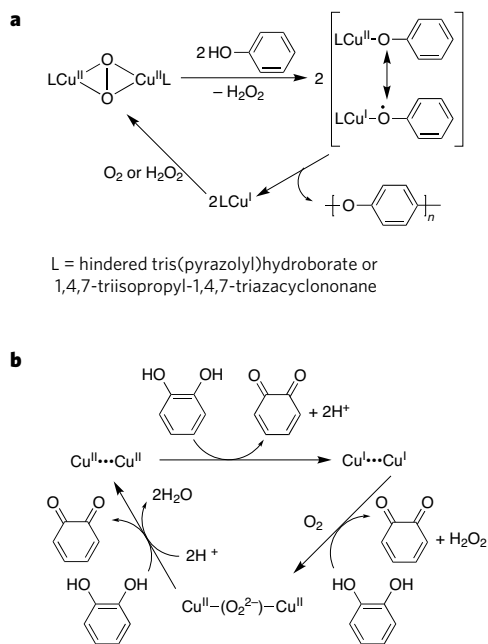


**Figure 7 | Oxidations by dicopper complexes.** **a**, The proposed catalytic cycle for the regio-controlled oxidative polymerization of phenols involves a (μ-η<sup>2</sup>:η<sup>2</sup>-peroxo)dicopper(II) model of the oxy forms of tyrosinase, haemocyanin and catechol oxidase. **b**, Multiple oxidation pathways have been proposed for the catalytic oxidation of catechols to *ortho*-quinones by dicopper complexes<sup>60</sup>.



**Table 1 | Iron and manganese oxidation catalysts that use H<sub>2</sub>O<sub>2</sub> as the oxidant to give high conversion of alkenes into epoxide or *cis*-diol products**

| Catalyst (mol%)                       | Additive (equivalents per metal)                             | Solvent (Temperature)                     | Alkene                 | H <sub>2</sub> O <sub>2</sub> :alkene | Epoxide yield | <i>cis</i> -Diol yield | Reference |
|---------------------------------------|--|---|------------------------|---------------------------------------|---------------|------------------------|-----------|
| Fe( <b>13</b> ) (0.05)                | None   | 3:1 MeOH:MeCN (25 °C)                     | Cyclooctene            | 1.2                                   | 95%           | 0%                     | 71        |
| Fe( <b>14</b> ) (1)                   | None   | CH <sub>2</sub> Cl <sub>2</sub> * (25 °C) | Cyclooctene            | 1                                     | 81%           | 0%                     | 72        |
| Fe( <b>17</b> ) (3)                   | None   | MeCN (25 °C)                              | 1-Octene               | 1.5                                   | 73%           | 3%                     | 84        |
| Fe( <b>17</b> ) (3)                   | HOAc (10)  | MeCN (25 °C)                              | 1-Decene               | 1.5                                   | 85%           | 0%                     | 83        |
| Fe( <b>17</b> ) (0.5)                 | HOAc (12,000)  | MeCN (0 °C)                               | Cyclooctene            | 1.5                                   | 99%           | <1%                    | 85        |
| Fe( <b>15</b> ) (3)                   | None   | MeCN (25 °C)                              | 1-Octene               | 4                                     | 16%           | 53%                    | 83        |
| Fe( <b>15</b> ) (0.5)                 | HOAc (12,000)  | MeCN (0 °C)                               | Cyclooctene            | 1.5                                   | 99%           | <1%                    | 85        |
| Fe( <b>16</b> ) (5)                   | None   | MeCN (25 °C)                              | Cyclooctene            | 1.5                                   | 9%            | 0%                     | 87        |
| Fe( <b>16</b> ) (5)                   | HOTf (5)   | MeCN (25 °C)                              | Cyclooctene            | 1.5                                   | 86%           | 0%                     | 87        |
| 1:2 FeCl <sub>3</sub> : <b>19</b> (5) | Pyrrolidine (2)  | <i>t</i> -AmylOH (25 °C)                  | <i>trans</i> -Stilbene | 2                                     | 97%           | 0%                     | 89        |
| MnSO <sub>4</sub> (1)                 | 0.2 M HCO <sub>3</sub> <sup>−</sup><br>pH 8 buffer (0.25)    | DMF (25 °C)                               | Cyclohexene            | 10                                    | 99%           | 0%                     | 92        |
| Mn( <b>20</b> ) (0.1)                 | None   | MeCN (0 °C)                               | Cyclooctene            | 1.3                                   | 1%            | 0.5%                   | 93        |
| Mn( <b>20</b> ) (0.1)                 | Cl <sub>3</sub> CCOOH (10)                                   | MeCN (0 °C)                               | Cyclooctene            | 1.3                                   | 24%           | 44%                    | 94        |
| Mn( <b>20</b> ) (0.1)                 | 2,6-Cl <sub>2</sub> C <sub>6</sub> H <sub>3</sub> -COOH (30) | MeCN (0 °C)                               | Cyclooctene            | 1.3                                   | 8%            | 53%                    | 94        |
| Mn( <b>20</b> ) (0.1)                 | Salicylic acid (50)  | MeCN (0 °C)                               | Cyclooctene            | 1.3                                   | 51%           | 13%                    | 94        |

\*In a biphasic mixture with the ionic liquid 1-butyl-3-methylimidazolium bromide. DMF, dimethylformamide; Me, methyl; OAc, acetate; OTf, trifluoromethanesulphonic acid.

or, more likely, undergo O–O bond cleavage to generate a high-valent iron–oxo species that contains the two oxidizing equivalents required to oxidize the substrate, the locations of which differ for each enzyme. The two oxidizing equivalents are distributed between the iron centre and the porphyrin ligand for cytochrome P450 and between the two iron centres in MMO, but must be localized on the mononuclear iron centre of the Rieske dioxygenases. There are thus several possible strategies for developing biomimetic catalysts. In this section, we focus on recent developments in iron catalysis using H<sub>2</sub>O<sub>2</sub> as an oxidant. From a biochemical perspective, these biologically inspired catalytic systems correspond to the peroxide shunt pathways that have been demonstrated for all three enzyme types and involve reactions of the iron(III) forms<sup>7,8,67,68</sup> of the enzymes with H<sub>2</sub>O<sub>2</sub>. The use of a combination of an iron salt or complex and H<sub>2</sub>O<sub>2</sub> as an oxidizing system has a history that dates back to the late nineteenth century<sup>69</sup>, but the major challenge has been to inhibit the homolytic cleavage of the peroxo O–O bond that produces non-selective, and thus unwanted, hydroxyl radicals. Instead, the aim is to direct the metal-promoted cleavage towards the generation of a metal-based oxidant that can carry out hydrocarbon oxidations with high chemo-, regio- and stereoselectivity<sup>7,8</sup>.

Much effort has been invested in the development of metalloporphyrin catalysts that mimic the reactivity of cytochrome P450, and these endeavours have been reviewed extensively<sup>70</sup>. The first two examples in Table 1 illustrate how efficiently H<sub>2</sub>O<sub>2</sub> can be converted into desired epoxide products by using electron-deficient porphyrins<sup>71,72</sup> (ligands are shown in Fig. 8). For the catalyst Fe(**13**), the solvent methanol provides the protons needed to promote the heterolytic cleavage of the peroxo O–O bond<sup>71,73</sup>, thereby mimicking a mechanistic principle well established for cytochrome P450 and related haem peroxidases<sup>7,74</sup>.

The marked increase in information on non-haem iron oxygenases within the past decade<sup>10,75,76</sup> has spurred efforts to explore the use of non-haem ligand scaffolds to facilitate such oxidation catalysis. Only recently have conditions been found to engender oxidative transformations with high stereoselectivity<sup>77–79</sup>. In this section, we highlight these notable successes in the epoxidation and *cis*-dihydroxylation of C=C bonds and the hydroxylation of aliphatic C–H bonds, which are all potentially important transformations in organic synthesis and medicinal chemistry.

The most extensively studied complexes thus far are those of tetradentate nitrogen-donor ligands with topologies that allow two *cis*-oriented coordination sites to be available for peroxide binding and activation. This arrangement is analogous to that found for the Rieske dioxygenases as illustrated by **3** (Fig. 2) but is in contrast to that typical for haem enzymes where only one coordination site is available for this purpose. A key observation that led to the discovery of this family of complexes

was the use of dilute H<sub>2</sub>O<sub>2</sub>, which minimized side reactions such as the unwanted production of highly reactive hydroxyl radicals<sup>80</sup>. When the reaction was carried out in this manner, compelling evidence for a metal-based oxidant was obtained. Specifically for the prototypical Fe(**15**) catalyst, cyclohexane oxidation resulted in a high alcohol:ketone product ratio that was unaffected by the presence of O<sub>2</sub>, and hydroxylation of the tertiary C–H bonds of *cis*-1,2-dimethylcyclohexane

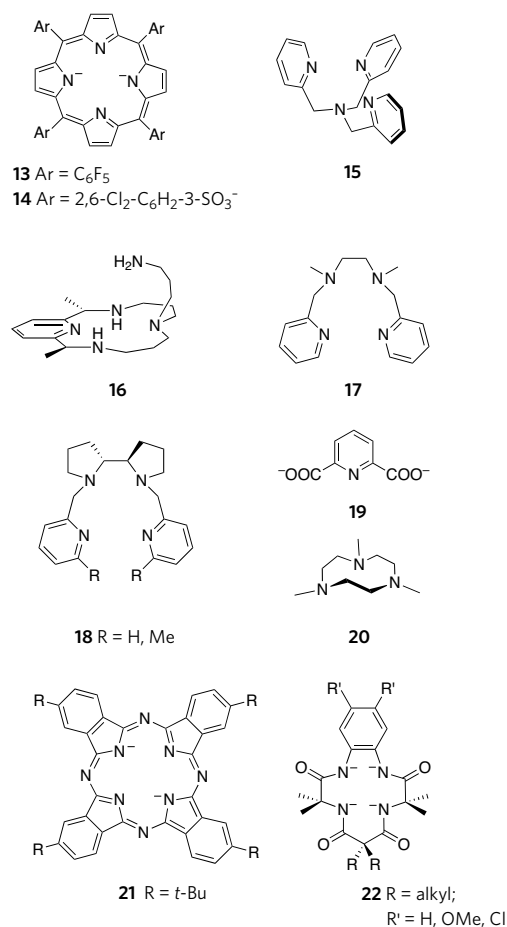


**Figure 8 | Ligands used for iron- and manganese-catalysed oxidations.** Many ligands, 13–22, have been used to support iron or manganese centres that catalyse the oxidation of hydrocarbons by H<sub>2</sub>O<sub>2</sub> (Table 1).

afforded a tertiary alcohol product with retention of configuration of the *cis*-1,2-dimethyl groups<sup>81</sup>. These results indicate a C–H bond cleavage event where alkyl radicals (if formed) are very short-lived. Oxidation of alkenes yielded epoxide and *cis*-diol products with similarly high retention of configuration<sup>82</sup>. Importantly, these reactions are the first examples of iron-catalysed *cis*-dihydroxylation of an alkene.

The nature of the metal-based oxidant in Fe(15) catalysis was deduced from a combination of low-temperature spectroscopic studies and room-temperature <sup>18</sup>O-labelling experiments<sup>81,82</sup>. At –40 °C an Fe(III)–OOH intermediate was trapped in acetonitrile (MeCN) solvent and characterized by a variety of spectroscopic methods; this intermediate was then proposed to undergo O–O bond cleavage to form the putative Fe(v)(O)(OH) oxidant. Strong support for the involvement of the latter came from labelling experiments that established the incorporation of added H<sub>2</sub><sup>18</sup>O into the oxidation products with retention of stereochemistry (Fig. 9). Most compelling was the observation that the *cis*-diol product incorporated one oxygen from H<sub>2</sub>O<sub>2</sub> and the other from H<sub>2</sub>O. These results emphasize the critical part a proximal proton donor (that is, the metal-bound water) plays in promoting the heterolytic cleavage of the O–O bond and rationalizes why complexes of closely related pentadentate ligands are poor catalysts for such oxidations.

So far, several non-haem iron-based catalytic oxidation systems have been developed with potential practical importance. Eric Jacobsen and co-workers demonstrated the use of acetic acid as an additive (30 mol%) in Fe(II)(17) catalysis that converted alkenes into epoxides with a high yield<sup>83</sup>. With 3 mol% catalyst and a 50% excess of H<sub>2</sub>O<sub>2</sub> at 4 °C, even terminal alkenes could be epoxidized to give product yields as high as 90%. The added acetic acid is clearly important, as this additive enhances both the yield and selectivity for epoxide<sup>83,84</sup>.

Further exploration of the effect of acetic acid in Fe(17) and Fe(15) catalysis by Rubén Mas-Ballesté and Lawrence Que Jr.<sup>85</sup> showed that cyclooctene could be converted nearly quantitatively to an epoxide within 2 min in a 1:2 MeCN:acetic acid solvent mixture at 0 °C. Spectroscopic and kinetic evidence was obtained for the binding of acetic acid to the Fe(III)–OOH intermediate, emphasizing the importance of a proximal proton donor to promote the heterolytic cleavage of the O–O bond to form an Fe(v)(O)(OAc) oxidant<sup>85,86</sup> (Fig. 9) and reiterating a principle well documented from studies of cytochrome P450 and haem peroxidases<sup>7,74</sup>. Similarly, Elena Rybak-Akimova and co-workers showed that the iron complex of macrocycle 16 (Fig. 8) became an effective epoxidation catalyst only when five equivalents of trifluoromethanesulphonic acid were added to the reaction mixture<sup>87</sup>. The added acid was proposed to protonate the aminoalkyl ‘tail’, generating an ammonium group close enough to a presumed Fe–OOH intermediate to promote heterolytic O–O bond cleavage.

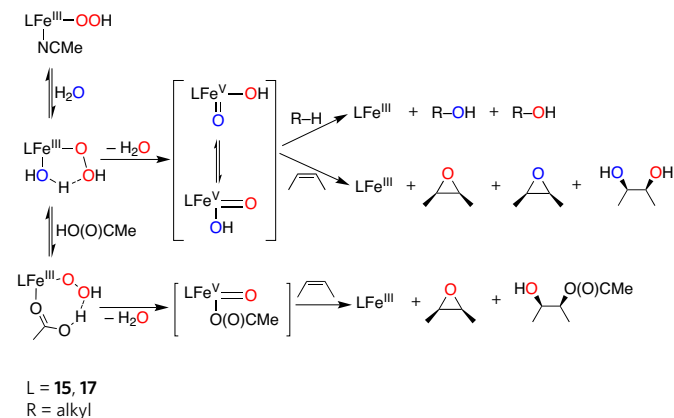


**Figure 9 | Mechanisms of oxidations by iron catalysts.** Proposed mechanisms for stereospecific oxidations of alkanes and alkenes by non-haem iron complexes invoke Fe(v)=O oxidants. Particularly instructive is the formation of a *cis*-diol from an alkene, with one oxygen atom from H<sub>2</sub>O<sub>2</sub> and the other from H<sub>2</sub>O. Oxygen atoms derived from H<sub>2</sub>O<sub>2</sub> (not depicted) are shown in red, and oxygen atoms derived from H<sub>2</sub>O are shown in blue. Me, methyl.

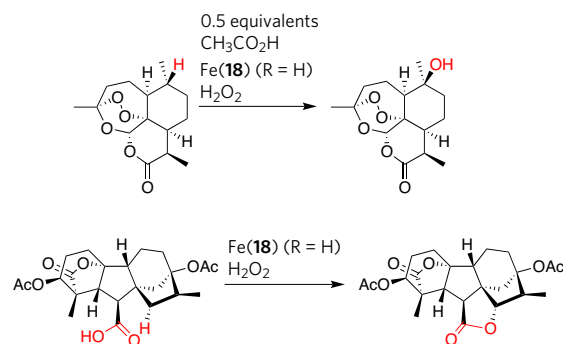


**Figure 10 | Illustrative selective oxidations by iron.** Highly selective oxidations of secondary and tertiary C–H bonds in complex natural products have been achieved using Fe(18) (R = H) and H<sub>2</sub>O<sub>2</sub>, as illustrated by the two reactions shown. The key functional groups involved are shown in red. Ac, acetyl.

Mark Chen and M. Christina White<sup>88</sup> have ingeniously applied the above Fe(17)–H<sub>2</sub>O<sub>2</sub>–acetic acid chemistry<sup>46</sup> to catalyse the hydroxylation of unactivated tertiary C–H bonds with a related Fe(18, where R is H) complex. With 5 mol% catalyst, the target C–H bond could be hydroxylated in 40–60% yield in many of the examples presented. In general, the most susceptible tertiary C–H bond is the one that is most electron-rich and least sterically hindered. The transformation was tolerant of many functional groups, as shown in Fig. 10 (upper panel) for the hydroxylation of the antimalarial drug artemisinin at the C10 position. When the substrate had a carboxylate functionality, the carboxylate took the place of the acetic acid additive and could be used to directly attack a nearby C–H bond, as illustrated in Fig. 10 (lower panel) for the hydroxylation of a tetrahydrogibberellic acid analogue. These examples show that these biologically inspired catalysts may be useful for the synthesis of complex organic molecules.

Iron complexes can also be used to catalyse asymmetric alkene oxidation, and two systems affording high enantioselectivity are mentioned here. Matthias Beller and co-workers developed an *in situ*-generated catalyst capable of epoxidizing aryl alkenes with up to 97% yield (Table 1) by using a combination of FeCl<sub>3</sub>, two equivalents of pyridine-2,6-carboxylic acid (the doubly protonated form of 19) and two equivalents of pyrrolidine in *tert*-amyl alcohol solvent<sup>89</sup>. When monotosylated (*S,S*)-1,2-diphenyldiaminoethane was used in place of pyrrolidine<sup>90</sup>, epoxides with an enantiomeric excess as high as 97% were obtained. By contrast, Que and co-workers used chiral ligand 18 (where R is Me) (Fig. 8) to obtain a complex that catalysed the oxidation of *trans*-2-heptene to give a *cis*-diol product with 97% enantiomeric excess<sup>91</sup>. Insights into the nature of the active species in these systems are not yet available.

Although not a strategy often used in nature, substituting Mn for Fe can result in superior oxidation catalysts, as was found for metalloporphyrins<sup>70</sup>. Non-porphyrinic Mn centres can also activate H<sub>2</sub>O<sub>2</sub> to catalyse alkene oxidations. Kevin Burgess and co-workers found that even simple MnSO<sub>4</sub> was effective for alkene epoxidation, when carried out in dimethylformamide (DMF) solvent in the presence of 0.2 M NaHCO<sub>3</sub> buffer at pH 8 (ref. 92). HCO<sub>4</sub><sup>–</sup> was formed under these conditions and presumably reacted with the Mn(II) ion to form either a Mn(II)–peroxocarbonato or Mn(IV)=O species that carried out the epoxidation. Ben Feringa and co-workers demonstrated that dinuclear Mn(20) complexes catalysed alkene oxidations with better turnover numbers than Fe(15) and Fe(17) (700 compared with 200 turnovers in the best-case scenarios)<sup>93,94</sup>. Both epoxide and *cis*-diol products were obtained, and the catalytic efficiency and the epoxide:diol ratio were modulated by the electronic and steric nature of carboxylic acid additives. Labelling studies of cyclooctene oxidation showed that H<sub>2</sub><sup>18</sup>O incorporation into epoxide and *cis*-diol products analogous to those reported for Fe(15), implicating the involvement of metal–peroxo and high-valent metal–oxo intermediates<sup>82</sup>. However, unlike in the iron study, the various species involved in Mn catalysis were proposed to be dinuclear in nature, and no intermediate has been identified so far<sup>94</sup>.

Very recently, it was reported that methane could be oxidized in water by  $\text{H}_2\text{O}_2$  at 25–60 °C with silica-supported  $[\text{Fe}_2\text{N}(\mathbf{21})_2]$  as the catalyst<sup>95</sup>. As many as 150 mols  $\text{CH}_4$  per mol catalyst could be oxidized to formaldehyde and formic acid. Catalytic activity was improved by the introduction of 0.1 M  $\text{H}_2\text{SO}_4$  and evidence was obtained for an  $\text{H}_2\text{O}_2$ -derived oxo adduct of the starting catalyst by electrospray mass spectrometry. On this basis, a mechanism following the haem paradigm (Fig. 1) was proposed involving formation of metal–peroxo and high-valent metal–oxo species on the intact Fe–N–Fe unit.

In closing, we briefly mention here the use of iron complex and  $\text{H}_2\text{O}_2$  combinations for environmental applications, which go beyond the scope of this review. This effort has been pioneered by Terrence Collins, whose group has designed and developed complexes of tetraamido macrocyclic ligands (TAML) such as **22** that are water-soluble and oxidatively and hydrolytically robust<sup>96</sup>. These complexes catalyse the activation of  $\text{H}_2\text{O}_2$  and are being investigated for use in the treatment of waste water from pulp and textile mills to remove coloured effluents and toxic chlorinated phenols. Although the nature of the oxidant(s) generated by the Fe(**22**) and  $\text{H}_2\text{O}_2$  combination that carry out these interesting transformations has not been established, metastable oxoiron(IV) and oxoiron(V) complexes of the TAML family have recently been trapped in organic solvents at low temperature and characterized spectroscopically<sup>97,98</sup>. Indeed, the latter is the only bona fide oxoiron(V) complex that has been identified.

## Challenges

In the past decade, Fe, Mn and Cu complexes with non-porphyrinic ligands that can catalyse oxidations of C–H and C=C bonds by  $\text{O}_2$  or  $\text{H}_2\text{O}_2$  have been identified. These oxidations were inspired by a mechanistic understanding of similar transformations carried out by iron and copper enzymes. The successes noted in this review are merely starting points for further investigations; much more work needs to be done to accomplish the goal of discovering broadly useful, active and highly selective hydrocarbon oxidation catalysts that operate in an environmentally friendly manner. With  $\text{H}_2\text{O}_2$  as the oxidant, appropriate conditions have been determined that minimize formation of unselective hydroxyl radicals and promote the heterolytic cleavage of the O–O bond. The latter generates a more selective metal-based oxidant that can effect substrate oxidations with significant chemoselectivity, regioselectivity, stereoselectivity and/or enantioselectivity. Putting this into practice in ways that are useful for industrial and fine-chemical synthesis is an important goal. Similarly, although effective catalysts for alcohol oxidations using copper–cofactor pairs have been developed, finding systems that are both highly active and broadly applicable requires further effort<sup>46</sup>. More generally, extending the range of substrates that can be oxidized under environmentally friendly conditions by iron or copper catalysts is an important goal, a prime example being the selective hydroxylation of methane to methanol performed by the soluble (di-iron-containing) and particulate (copper-containing) MMOs<sup>10,99</sup>.

A significant challenge is the development of selective catalytic systems that use  $\text{O}_2$  as the oxidant and avoid deleterious side reactions. Biological systems have unique capabilities in this regard through the control of the spatial and/or temporal distribution of substrates and oxidants. Such control has yet to be exerted in model systems and needs to be addressed, perhaps through more sophisticated biomimetic design strategies than those used so far. Further discoveries are likely to be made as mechanistic understanding of the enzymes accrues, new types of reactive intermediate in the biological and synthetic models systems are uncovered and applications toward catalysis are explored. ■

- Arakawa, H. *et al.* Catalysis research of relevance to carbon management: progress, challenges, and opportunities. *Chem. Rev.* **101**, 953–996 (2001).
- Punniyamurthy, T., Velusamy, S. & Iqbal, J. Recent advances in transition metal catalyzed oxidation of organic substrates with molecular oxygen. *Chem. Rev.* **105**, 2329–2364 (2005).
- Conley, B. L. *et al.* In *Activation of Small Molecules: Organometallic and Bioinorganic Perspectives* (ed. Tolman, W. B.) 235–285 (Wiley-VCH, 2006).
- Meunier, B. (ed.) *Biomimetic Oxidations Catalyzed by Transition Metal Complexes* (Imperial College Press, 2000).
- Mahadevan, V., Klein Gebbink, R. J. M. & Stack, T. D. P. Biomimetic modeling of copper oxidase reactivity. *Curr. Opin. Chem. Biol.* **4**, 228–234 (2000).
- Sheldon, R. A., Arends, I. & Hanefeld, U. *Green Chemistry and Catalysis* (Wiley-VCH, 2007).
- Denisov, I. G., Makris, T. M., Sligar, S. G. & Schlichting, I. Structure and chemistry of cytochrome P450. *Chem. Rev.* **105**, 2253–2278 (2005).
- Dawson, J. H. Probing structure–function relations in heme-containing oxygenases and peroxidases. *Science* **240**, 433–439 (1988).
- Que, L. The heme paradigm revisited: alternative reaction pathways considered. *J. Biol. Inorg. Chem.* **9**, 643–690 (2004).
- Merkx, M. *et al.* Dioxxygen activation and methane hydroxylation by soluble methane monooxygenase: a tale of two irons and three proteins. *Angew. Chem. Int. Edn Engl.* **40**, 2782–2807 (2001).
- Beauvais, L. G. & Lippard, S. J. Reactions of the peroxo intermediate of soluble methane monooxygenase hydroxylase with ethers. *J. Am. Chem. Soc.* **127**, 7370–7378 (2005).
- Waller, B. J. & Lipscomb, J. D. Dioxxygen activation by enzymes containing binuclear non-heme iron clusters. *Chem. Rev.* **96**, 2625–2658 (1996).
- Shu, L. *et al.* An  $\text{Fe}_2^{IV}\text{O}_2$  diamond core structure for the key intermediate Q of methane monooxygenase. *Science* **275**, 515–518 (1997).
- Ferraro, D. J., Gakhar, L. & Ramaswamy, S. Rieske business: structure–function of Rieske non-heme oxygenases. *Biochem. Biophys. Res. Commun.* **338**, 175–190 (2005).
- Karlsson, A. *et al.* Side-on binding of dioxxygen to iron: implications for enzymatic cis-dihydroxylation reactions. *Science* **299**, 1039–1042 (2003).
- Krebs, C., Galonic Fujimori, D., Walsh, C. T. & Bollinger, J. M. Jr. Non-heme Fe(IV)–oxo intermediates. *Acc. Chem. Res.* **40**, 484–492 (2007).
- Solomon, E. I., Chen, P., Metz, M., Lee, S.-K. & Palmer, A. E. Oxygen binding, activation, and reduction to water by copper proteins. *Angew. Chem. Int. Edn Engl.* **40**, 4570–4590 (2001).
- Whittaker, J. W. Free radical catalysis by galactose oxidase. *Chem. Rev.* **103**, 2347–2363 (2003).
- Whittaker, J. W. The radical chemistry of galactose oxidase. *Arch. Biochem. Biophys.* **433**, 227–239 (2005).
- Ito, N. *et al.* Novel thioether bond revealed by a 1.7 Å crystal structure of galactose oxidase. *Nature* **350**, 87–90 (1991).
- Rogers, M. S. *et al.* The stacking tryptophan of galactose oxidase: a second-coordination sphere residue that has profound effects on tyrosyl radical behavior and enzyme catalysis. *Biochemistry* **46**, 4606–4618 (2007).
- Jazdzewski, B. A. & Tolman, W. B. Understanding the copper-phenoxyl radical array in galactose oxidase: contributions from synthetic modeling studies. *Coord. Chem. Rev.* **200–202**, 633–685 (2000).
- Fabrice, T. Ten years of a biomimetic approach to the copper(II) radical site of galactose oxidase. *Eur. J. Inorg. Chem.* **2007**, 2379–2404 (2007).
- Rokhsana, D., Dooley, D. M. & Szilagyi, R. K. Systematic development of computational models for the catalytic site in galactose oxidase: impact of outer-sphere residues on the geometric and electronic structures. *J. Biol. Inorg. Chem.* **13**, 371–383 (2008).
- Whittaker, M. M. & Whittaker, J. W. Catalytic reaction profile for alcohol oxidation by galactose oxidase. *Biochemistry* **40**, 7140–7148 (2001).
- Magnus, K. A., Ton-That, H. & Carpenter, J. E. Recent structural work on the oxygen transport protein hemocyanin. *Chem. Rev.* **94**, 727–735 (1994).
- Cuff, M. E., Miller, K. I., van Holde, K. E. & Hendrickson, W. A. Crystal structure of a functional unit from octopus hemocyanin. *J. Mol. Biol.* **278**, 855–870 (1998).
- Matoba, Y., Kumagai, T., Yamamoto, A., Yoshitsu, H. & Sugiyama, M. Crystallographic evidence that the dinuclear copper center of tyrosinase is flexible during catalysis. *J. Biol. Chem.* **281**, 8981–8990 (2006).
- Rompel, A. *et al.* Purification and spectroscopic studies on catechol oxidases from *Lycopus europaeus* and *Populus nigra*: evidence for a dinuclear copper center of type 3 and spectroscopic similarities of tyrosinase and hemocyanin. *J. Biol. Inorg. Chem.* **4**, 56–63 (1999).
- Granata, A., Monzani, E., Bubacco, L. & Casella, L. Mechanistic insight into the activity of tyrosinase from variable-temperature studies in an aqueous/organic solvent. *Chem. Eur. J.* **12**, 2504–2514 (2006).
- Yamazaki, S. & Itoh, S. Kinetic evaluation of phenolase activity of tyrosinase using simplified catalytic reaction system. *J. Am. Chem. Soc.* **125**, 13034–13035 (2003).
- Mirica, L. M., Ottenwaelde, X. & Stack, T. D. P. Structure and spectroscopy of copper-dioxxygen complexes. *Chem. Rev.* **104**, 1013–1045 (2004).
- Lewis, E. A. & Tolman, W. B. Reactivity of copper-dioxxygen systems. *Chem. Rev.* **104**, 1047–1076 (2004).
- Hatcher, L. Q. & Karlin, K. D. Ligand influences in copper-dioxxygen complex-formation and substrate oxidations. *Adv. Inorg. Chem.* **58**, 131–184 (2006).
- Mirica, L. M. *et al.* Tyrosinase reactivity in a model complex: an alternative hydroxylation mechanism. *Science* **308**, 1890–1892 (2005).
- Brazeau, B. J., Johnson, B. J. & Wilmot, C. M. Copper-containing amine oxidases. Biogenesis and catalysis: a structural perspective. *Arch. Biochem. Biophys.* **428**, 22–31 (2004).
- Klinman, J. P. The copper-enzyme family of dopamine β-monooxygenase and peptidylglycine α-hydroxylating monooxygenase: resolving the chemical pathway for substrate hydroxylation. *J. Biol. Chem.* **281**, 3013–3016 (2006).
- Evans, J. P., Ahn, K. & Klinman, J. P. Evidence that dioxygen and substrate activation are tightly coupled in dopamine β-monooxygenase: implications for the reactive oxygen species. *J. Biol. Chem.* **278**, 49691–49698 (2003).
- Chen, P. & Solomon, E. I. Oxygen activation by the noncoupled binuclear copper site in peptidylglycine α-hydroxylating monooxygenase. Reaction mechanism and role of the noncoupled nature of the active site. *J. Am. Chem. Soc.* **126**, 4991–5000 (2004).
- Cramer, C. J. & Tolman, W. B. Mononuclear  $\text{CuO}_2$  complexes: geometries, spectroscopic properties, electronic structures, and reactivity. *Acc. Chem. Res.* **40**, 601–608 (2007).
- Prigge, S. T., Eipper, B. A., Mains, R. E. & Amzel, L. M. Dioxxygen binds end-on to mononuclear copper in a precatalytic enzyme complex. *Science* **304**, 864–867 (2004).
- Yoshizawa, K., Kihara, N., Kamachi, T. & Shiota, Y. Catalytic mechanism of dopamine β-monooxygenase mediated by  $\text{Cu(III)}$ -oxo. *Inorg. Chem.* **45**, 3034–3041 (2006).



43. Crespo, A., Marti, M. A., Roitberg, A. E., Amzel, L. M. & Estrin, D. A. The catalytic mechanism of peptidylglycine  $\alpha$ -hydroxylating monooxygenase investigated by computer simulation. *J. Am. Chem. Soc.* **128**, 12817–12828 (2006).
44. Rolff, M. & Tuzcek, F. How do copper enzymes hydroxylate aliphatic substrates? Recent insights from the chemistry of model systems. *Angew. Chem. Int. Edn Engl.* **47**, 2344–2347 (2008).
45. Punniyamoorthy, T. & Rout, L. Recent advances in copper-catalyzed oxidation of organic compounds. *Coord. Chem. Rev.* **252**, 134–154 (2008).
46. Arends, I., Gamez, P. & Sheldon, R. A. Green oxidation of alcohols using biomimetic Cu complexes and Cu enzymes as catalysts. *Adv. Inorg. Chem.* **58**, 235–279 (2006).  
**This review surveys progress in the use of biologically inspired copper-ligand radical complexes as alcohol oxidation catalysts.**
47. Piera, J. & Bäckvall, J. E. Catalytic oxidation of organic substrates by molecular oxygen and hydrogen peroxide by multistep electron transfer — a biomimetic approach. *Angew. Chem. Int. Edn Engl.* **47**, 3506–3523 (2008).  
**This topical review on biologically inspired oxidation catalysis emphasizes systems that use electron-transfer mediators to couple reduction and oxidation steps in biomimetic catalytic cycles.**
48. Wang, Y. & Stack, T. D. P. Galactose oxidase model complexes: catalytic reactivities. *J. Am. Chem. Soc.* **118**, 13097–13098 (1996).
49. Wang, Y., DuBois, J. L., Hedman, B., Hodgson, K. O. & Stack, T. D. P. Catalytic galactose oxidase models: biomimetic Cu(II)-phenoxyl-radical reactivity. *Science* **279**, 537–540 (1998).
50. Chaudhuri, P. *et al.* Biomimetic metal-radical reactivity: aerial oxidation of alcohols, amines, aminophenols and catechols catalyzed by transition metal complexes. *J. Biol. Chem.* **386**, 1023–1033 (2005).
51. Chaudhuri, P., Hess, H., Flörke, U. & Wiegardt, K. From structural models of galactose oxidase to homogeneous catalysis: efficient aerobic oxidation of alcohols. *Angew. Chem. Int. Edn Engl.* **37**, 2217–2220 (1998).
52. Chaudhuri, P., Hess, M., Weyhermüller, T. & Wiegardt, K. Aerobic oxidation of primary alcohols by a new mononuclear Cu(II)-radical catalyst. *Angew. Chem. Int. Edn Engl.* **38**, 1095–1098 (1999).
53. Chaudhuri, P. *et al.* Aerobic oxidation of primary alcohols (including methanol) by copper(II)- and zinc(II)-phenoxyl radical catalysts. *J. Am. Chem. Soc.* **121**, 9599–9610 (1999).
54. Paine, T. K., Weyhermüller, T., Wiegardt, K. & Chaudhuri, P. Aerial oxidation of primary alcohols and amines catalyzed by Cu(II) complexes of 2,2'-selenobis(4,6-di-*tert*-butylphenol) providing [O,Se,O]-donor atoms. *Dalton Trans.* 2092–2101 (2004).
55. Sheldon, R. & Arends, I. Catalytic oxidations mediated by metal ions and nitroxyl radicals. *J. Mol. Catal. A* **251**, 200–214 (2006).
56. Jiang, N. & Ragauskas, A. J. Copper(II)-catalyzed aerobic oxidation of primary alcohols to aldehydes in ionic liquid [bmpp]PF<sub>6</sub>. *Org. Lett.* **7**, 3689–3692 (2005).
57. Ragagnin, G., Betzemeier, B., Quici, S. & Knochel, P. Copper-catalysed aerobic oxidation of alcohols using fluorous biphasic catalysis. *Tetrahedron* **58**, 3985–3991 (2002).
58. Markó, I. E. *et al.* Efficient, ecologically benign, aerobic oxidation of alcohols. *Adv. Inorg. Chem.* **56**, 211–240 (2004).
59. Markó, I. *et al.* Efficient, copper-catalyzed, aerobic oxidation of primary alcohols. *Angew. Chem. Int. Edn Engl.* **43**, 1588–1591 (2004).
60. Battaini, G., Granata, A., Monzani, E., Gullotti, M. & Casella, L. Biomimetic oxidations by dinuclear and trinuclear copper complexes. *Adv. Inorg. Chem.* **58**, 185–233 (2006).
61. Koval, I. A., Gamez, P., Belle, C., Selmeçci, K. & Reedijk, J. Synthetic models of the active site of catechol oxidase: mechanistic studies. *Chem. Soc. Rev.* **35**, 814–840 (2006).  
**References 60 and 61 review the catalytic oxidations of phenols and catechols by synthetic models of the dicopper active sites of tyrosinase and catechol oxidase from a mechanistic perspective.**
62. Higashimura, H. *et al.* Highly regioselective oxidative polymerization of 4-phenoxyphenol to poly(1,4-phenylene oxide) catalyzed by tyrosinase model complexes. *J. Am. Chem. Soc.* **120**, 8529–8530 (1998).
63. Higashimura, H. *et al.* 'Radical-controlled' oxidative polymerization of 4-phenoxyphenol by a tyrosinase model complex catalyst to poly(1,4-phenylene oxide). *Macromolecules* **33**, 1986–1995 (2000).
64. Higashimura, H. *et al.* 'Radical-controlled' oxidative polymerization of *o*-cresol catalyzed by  $\mu$ - $\eta^2$ - $\eta^2$ -peroxo dicopper(II) complex. *Appl. Catal. A* **194**, 427–433 (2000).
65. Higashimura, H., Fujisawa, K., Kubota, M. & Kobayashi, S. 'Radical-controlled' oxidative polymerization of phenol: Comparison with that of 4-phenoxyphenol. *J. Polym. Sci. Polym. Chem.* **43**, 1955–1962 (2005).
66. Shibasaki, Y., Suzuki, Y. & Ueda, M. Copper-catalyzed regio-controlled oxidative coupling polymerization of 2,5-dimethylphenol. *Macromolecules* **40**, 5322–5325 (2007).
67. Andersson, K. K., Froland, W. A., Lee, S.-K. & Lipscomb, J. D. Dioxygen independent oxygenation of hydrocarbons by methane monooxygenase hydroxylase component. *New J. Chem.* **15**, 411–415 (1991).
68. Wolfe, M. D. & Lipscomb, J. D. Hydrogen peroxide-coupled *cis*-diol formation catalyzed by naphthalene 1,2-dioxygenase. *J. Biol. Chem.* **278**, 829–835 (2003).
69. Fenton, H. J. H. Oxidation of tartaric acid in the presence of iron. *J. Chem. Soc.* **65**, 889–910 (1894).
70. Meunier, B., Robert, A., Pratiel, G. & Bernadou, J. In *The Porphyrin Handbook* (eds Kadish, K. M., Smith, K. M. & Guillard, R.) 119–187 (Academic, 2000).
71. Nam, W. *et al.* Factors affecting the catalytic epoxidation of olefins by iron porphyrin complexes and H<sub>2</sub>O<sub>2</sub> in protic solvents. *J. Org. Chem.* **68**, 7903–7906 (2007).
72. Srinivas, K. A., Kumar, A. & Chauhan, M. S. Epoxidation of alkenes with hydrogen peroxide catalyzed by iron(III) porphyrins in ionic liquids. *Chem. Commun.* 2456–2457 (2002).
73. Stephenson, N. A. & Bell, A. T. A study of the mechanism and kinetics of cyclooctene epoxidation catalyzed by iron(III) tetrakis(pentafluorophenyl) porphyrin. *J. Am. Chem. Soc.* **127**, 8635–8643 (2005).
74. Sono, M., Roach, M. P., Coulter, E. D. & Dawson, J. H. Heme-containing oxygenases. *Chem. Rev.* **96**, 2841–2887 (1996).
75. Abu-Omar, M. M., Loaiza, A. & Hontzeas, N. Reaction mechanisms of mononuclear non-heme iron oxygenases. *Chem. Rev.* **105**, 2227–2252 (2005).
76. Costas, M., Mehn, M. P., Jensen, M. P. & Que, L. Jr. Oxygen activation at mononuclear nonheme iron: Enzymes, intermediates, and models. *Chem. Rev.* **104**, 939–986 (2004).
77. Costas, M., Chen, K. & Que, L. Jr. Biomimetic nonheme iron catalysts for alkane hydroxylation. *Coord. Chem. Rev.* **200–202**, 517–544 (2000).
78. Lane, B. S. & Burgess, K. Metal-catalyzed epoxidations of alkenes with hydrogen peroxide. *Chem. Rev.* **103**, 2457–2474 (2003).
79. Tanase, S. & Bouwman, E. Selective conversion of hydrocarbons with H<sub>2</sub>O<sub>2</sub> using biomimetic non-heme iron and manganese oxidation catalysts. *Adv. Inorg. Chem.* **58**, 29–75 (2006).
80. Chen, K., Costas, M. & Que, L. Jr. Spin state tuning of non-heme iron-catalyzed hydrocarbon oxidations: Participation of Fe<sup>III</sup>-OOH and Fe<sup>V</sup>=O intermediates. *Dalton Trans.* 672–679 (2002).
81. Chen, K. & Que, L. Jr. Stereospecific alkane hydroxylation by nonheme iron catalysts: Mechanistic evidence for an Fe<sup>V</sup>=O active species. *J. Am. Chem. Soc.* **123**, 6327–6337 (2001).
82. Chen, K., Costas, M., Kim, J., Tipton, A. K. & Que, L. Jr. Olefin *cis*-dihydroxylation versus epoxidation by nonheme iron catalysts: two faces of an Fe<sup>III</sup>-OOH coin. *J. Am. Chem. Soc.* **124**, 3026–3035 (2002).  
**This paper summarizes the mechanistic arguments in favour of the formation of the Fe(V)=O species shown in Fig. 9 that are responsible for highly stereoselective alkene oxidations by H<sub>2</sub>O<sub>2</sub>, that are catalysed by non-haem iron complexes.**
83. White, M. C., Doyle, A. G. & Jacobsen, E. N. A synthetically useful, self-assembling MMO mimic system for catalytic alkene epoxidation with aqueous H<sub>2</sub>O<sub>2</sub>. *J. Am. Chem. Soc.* **123**, 7194–7195 (2001).
84. Ryu, J. Y. *et al.* High conversion of olefins to *cis*-diols by non-heme iron catalysts and H<sub>2</sub>O<sub>2</sub>. *Chem. Commun.* 1288–1289 (2002).
85. Mas-Ballester, R. & Que, L. Jr. Iron-catalyzed olefin epoxidation in the presence of acetic acid: Insights into the nature of the metal-based oxidant. *J. Am. Chem. Soc.* **129**, 15964–15972 (2007).
86. Mas-Ballester, R., Fujita, M., Que, L. Jr. High-valent iron-mediated *cis*-hydroxyacetoxylation of olefins. *Dalton Trans.* 1828–1830 (2008).
87. Taktak, S., Ye, W., Herrera, A. M. & Rybak-Akimova, E. V. Synthesis and catalytic properties in olefin epoxidation of novel iron(II) complexes with pyridine-containing macrocycles bearing an aminopropyl pendant arm. *Inorg. Chem.* **46**, 2929–2942 (2007).
88. Chen, M. S. & White, M. C. A predictably selective aliphatic C–H oxidation reaction for complex molecule synthesis. *Science* **318**, 783–787 (2007).  
**This paper shows that the non-haem iron complex Fe(18) can generate an oxidant from H<sub>2</sub>O<sub>2</sub> that selectively hydroxylates particular tertiary C–H bonds in complex organic molecules.**
89. Anilkumar, G., Bitterlich, B., Gelalcha, F. G., Tse, M. K. & Beller, M. An efficient biomimetic Fe-catalyzed epoxidation of olefins using hydrogen peroxide. *Chem. Commun.* 289–291 (2007).
90. Gelalcha, F. G., Bitterlich, B., Anilkumar, A., Tse, M. K. & Beller, M. Iron-catalyzed asymmetric epoxidation of aromatic alkenes using hydrogen peroxide. *Angew. Chem. Int. Edn Engl.* **46**, 7293–7296 (2007).  
**This paper reports the highest enantioselectivity so far for the epoxidation of an alkene by a non-haem iron catalyst.**
91. Suzuki, K., Oldenburg, P. D. & Que, L. Jr. Iron-catalyzed asymmetric olefin *cis*-dihydroxylation with 97% enantiomeric excess. *Angew. Chem. Int. Edn Engl.* **47**, 1887–1889 (2008).  
**This paper reports the highest enantioselectivity so far for the *cis*-dihydroxylation of an alkene by a non-haem iron catalyst.**
92. Lane, B. S., Vogt, M., DeRose, V. J. & Burgess, K. Manganese-catalyzed epoxidations of alkenes in bicarbonate solutions. *J. Am. Chem. Soc.* **124**, 11946–11954 (2002).
93. de Boer, J. W. *et al.* *cis*-Dihydroxylation and epoxidation of alkenes by [Mn<sub>2</sub>O(OCO)<sub>2</sub>(tmtacn)<sub>2</sub>]: Tailoring the selectivity of a highly H<sub>2</sub>O<sub>2</sub>-efficient catalyst. *J. Am. Chem. Soc.* **127**, 7990–7991 (2005).
94. de Boer, J. W. *et al.* Mechanism of *cis*-dihydroxylation and epoxidation of alkenes by highly H<sub>2</sub>O<sub>2</sub> efficient dinuclear manganese catalysts. *Inorg. Chem.* **46**, 6353–6372 (2007).
95. Sorokin, A. B., Kudrik, E. V. & Bouchu, D. Bio-inspired oxidation of methane in water catalyzed by N-bridged diiron phthalocyanine complex. *Chem. Commun.* 2562–2564 (2008).  
**This paper demonstrates the iron-catalysed oxidation of methane by H<sub>2</sub>O<sub>2</sub> at relatively mild temperatures (<100 °C).**
96. Collins, T. J. TAML oxidant activators: A new approach to the activation of hydrogen peroxide for environmentally significant problems. *Acc. Chem. Res.* **35**, 782–790 (2002).  
**This review summarizes the work of Collins's group in the use of Fe(TAML) complexes as effective catalysts for H<sub>2</sub>O<sub>2</sub> activation in the treatment of waste water from paper and textile mills.**
97. Chanda, A. *et al.* (TAML)Fe<sup>V</sup>=O complex in aqueous solution: Synthesis and spectroscopic and computational characterization. *Inorg. Chem.* **47**, 3669–3678 (2008).
98. Tiago de Oliveira, F. *et al.* Chemical and spectroscopic evidence for an Fe<sup>V</sup>-oxo complex. *Science* **315**, 835–838 (2007).
99. Balasubramanian, R. & Rosenzweig, A. Structural and mechanistic insights into methane oxidation by particulate methane monooxygenase. *Acc. Chem. Res.* **40**, 573–580 (2007).

**Acknowledgements** Work on biologically inspired oxidation catalysis carried out in the laboratory of L.Q. is supported by the US Department of Energy, and support for copper oxidation chemistry in the laboratory of W.B.T. is provided by the National Institutes of Health.

**Author Information** Reprints and permissions information is available at [www.nature.com/reprints](http://www.nature.com/reprints). The authors declare no competing financial interests. Correspondence should be addressed to the authors (larryque@umn.edu; wtolman@umn.edu).